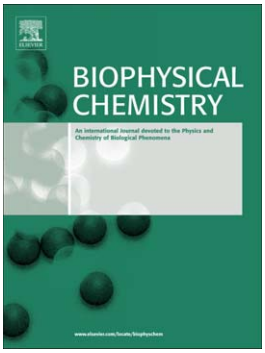

Thermal aggregation of β-lactoglobulin in presence of metal ions

Giovanna Navarra, Maurizio Leone, Valeria Militello

PII: S0301-4622(07)00204-9
DOI: doi: 10.1016/j.bpc.2007.09.003
Reference: BIOCHE 5015

To appear in: *Biophysical Chemistry*

Received date: 25 July 2007
Revised date: 5 September 2007
Accepted date: 5 September 2007

Please cite this article as: Giovanna Navarra, Maurizio Leone, Valeria Militello, Thermal aggregation of β-lactoglobulin in presence of metal ions, *Biophysical Chemistry* (2007), doi: 10.1016/j.bpc.2007.09.003

Thermal aggregation of β-lactoglobulin in presence of metal ions

Giovanna Navarra, Maurizio Leone and Valeria Militello

Università di Palermo, Dipartimento di Scienze Fisiche ed Astronomiche
Via Archirafi 36 Palermo, Italy
Consiglio Nazionale delle Ricerche, Istituto di Biofisica, U. O. di Palermo

Corresponding author:

Valeria Militello
Dipartimento di Scienze Fisiche e Astronomiche, Via Archirafi 36
90123 Palermo, Italy.
E-mail: militello@fisica.unipa.it
Phone: +39-091-6234299
Fax: +39-091-6234281

Abstract

In this work, we report a study on the effects of zinc and copper ions on the heat-induced aggregation of β–Lactoglobulin (BLG). Kinetics investigations on aggregates growth by light scattering measurements and on secondary structure changes by FT-IR absorption measurements show the different role played by two metals during the whole process. In particular, the presence of zinc in solution promotes the formation of aggregates of BLG at a lower temperature than the copper. Then, fixed the temperature, formation of a large amount of aggregates, with a large dimension, is observed for the Zn-BLG in shorter time; on the contrary, the presence of the copper in solution does not affect the aggregation process but the secondary structure changes and the formation of different stronger intermolecular H-bonds, which probably lead to build a network of bonds that takes towards gelation. Our studies show as time evolution of aggregation process of BLG is dramatically affected by the presence of metal ions in solution and structural protein modifications are induced by different divalent metal ions.

Keywords: beta-lactoglobulin, protein aggregation, metal ions, light scattering, FTIR spectroscopy

1. Introduction

In the last years, it has been observed and studied the aggregation process induced by metal ions, for biomedical and biotechnological purposes. The first of these two aspects is related to studies on several protein systems, most of them on beta amyloid peptide, involved in protein deposition diseases. The idea arises from the finding that increased metal concentrations (mainly copper, iron and zinc) were present in the brains of Alzheimer's disease patients both in the amyloid plaques and in the cortical tissue [1-3]. Cu^{2+} and Zn^{2+} metals ions have a different physiological role and it has been observed that, in vitro, both promote (more zinc than copper) aggregation in amyloid fibrils and/or in amorphous aggregates [4-11]. Then, as a function of parameters like solvent's pH and metal concentration, these two ions have shown different behaviors; in particular, under physiological conditions, the amyloid peptide has a higher propensity to bind zinc, whereas, under mildly acidic conditions, as in physiological acidosis following an inflammatory process, copper is preferentially bound; in other words, zinc can protect against copper toxicity, which is induced by acidosis [12,13]. In addition, studies with different concentrations of copper and zinc have shown that these metals prevent fibril formation of amyloid peptide by promoting the formation of no fibril aggregates [8,14-16], like oligomeric aggregates that are more neurotoxic than the same fibrils [17-24]. Finally, other results obtained by structural studies, have shown that this peptide has two metal binding sites with higher and lower affinity: copper in high affinity site is coordinated in a planar configuration with three histidines and terminus or Tyr10 and this binding site is able to bind also a zinc ion [21,22,25]. The four aminoacids proposed for zinc binding site are Tyr10, Glu11, Arg5 or the N-terminus [6,26-29]. It has been made hypothesis about the presence for both metals in the second low affinity binding site but it is still studying [30-32]. More recently, it has also been reported that alterations in the disposition of zinc ions may be important in the initiation and development of amyotrophic lateral sclerosis. In particular, alterations in the expression of metallothioneins, which regulate cellular levels of zinc, have been reported in mutant superoxide

dismutase SOD1 mice: deletion of metallothioneins in these animals accelerates disease progression [33].

The second purpose of the scientific interest, in studying aggregation protein process, drops in the field of biotechnologies as food technology. In fact, most processes in manufacturing of foods are based on thermal treatments. To know the structures of the proteins during and after these treatments is extremely important also for allergenic problems. Regarding dairy production, milk proteins are much studied because some of them are major constituent of fouling deposits in the dairy industry [34]. For example, casein, that is the most predominant phosphoprotein found in milk and cheese as a suspension of particles called casein micelles, binds zinc atoms [35], while β-lactoglobulin (BLG) chelates calcium and precipitates when heated and as a function of pH [36]. Moreover, in mixtures of whey proteins, fibril-like aggregates have been found [37,38] as in production of gels or aggregates in presence of calcium or zinc, respectively [39-41]. In fact, metal ions are also able to induce cold gelation and the gel texture formation depends on different parameters as pH conditions and protein and/or iron concentration [42,43]. Therefore, protein aggregation is important in food processing and it is relevant to know how aggregation of food proteins occurs and if it is a source of amyloid fibrils [44].

We have already studied thermal induced aggregation of several proteins and we have shown that the whole process is accompanied by significant changes in the conformation and structure of the native molecule [45-49]. Here, we will show, applying the same approach, the study of the aggregation of BLG in presence of copper and zinc in solution. We have selected the BLG because of its double interest above mentioned, as a model beta-protein in the aggregation process and as a thermal marker in the industrial processes involved in preparation of milk [50]. In general, BLG is the major whey protein of ruminant species and is present in the milk of many, but not all, other species. The protein family to which BLG belongs, the lipocalins [51], presents a widely diverse series of functions, most of which involve some ligand-binding function; it has been speculated that this binding-function must be the physiological reason for the significant quantities of BLG found

in milk. This globular protein consists of 162 aminoacids (18,4 kDa) and is a dimer at neutral pH; it has a core structural pattern formed by one α-helix and eight strands of antiparallel β-sheets and its tertiary structure is stabilized from two disulfide bonds. Moreover, there is also one free SH group (pKa = 8), corresponding to Cys-121, buried in the hydrophobic core of the protein [52–56]. It is a protein extremely sensitive to thermal denaturation [57] and has a mild antioxidant nature due to the free thiol group [58]. In fact, it is already reported that, when heated, globular proteins tend to aggregate, thanks to the contribution of intermolecular disulfide bonds [7,25,27,28] and hydrophobic interactions [47]. In particular, when the temperature increases, monomerization and partial unfolding of the protein are induced with consequent exposure of SH group and formation of an intermolecular bond with a free cysteine of a close molecule. The disulfide exchange can also be promoted in smaller way when the pH value decreases and when the BLG is partly denatured [42,43].

To get more insight into the role of the metal ions on the aggregation, here we report a study on the effects of Cu^{2+} and Zn^{2+} on the heat-induced aggregation of BLG, at pH 7 and at temperature of 60 °C. We monitor the time evolution of the mean dimension of the aggregates by dynamic light scattering measurements; while, structural and conformational changes at secondary and tertiary level respectively, are followed by time evolution of Amide I' and Amide II bands profiles, monitored by infrared absorption spectroscopy. Amide I' is a probe of protein structural organization in terms of α-helix, random coil and β-sheet contents and gives information on intermolecular aggregation through the appearance of two shoulders attributed to β-sheet formation [44,60-63]. Amide II is a probe of partial opening of the tertiary structure, which allows the H-D exchange of those hydrogens entrapped in the core of protein before opening [47].

2. Materials and methods

2.1. Samples preparation

β-lactoglobulin A from bovine milk was obtained from Sigma-Aldrich. Powdered protein was dissolved in a 20 mM MES buffer prepared in D_2O (99.9%, Aldrich) and titred with KOH until to pD 7 (where pD is pH meter reading + 0.4 correction). The final concentration of protein was 3.3 mM. $CuCl_2$ and $ZnCl_2$ (99.999%, Sigma-Aldrich) 0.1 M were diluted in buffer at 1% and their final concentration was 1 mM. The freshly prepared samples, centrifuged (2000 rpm for 8 minutes) and filtered (0.20 μm), were divided in two aliquots for IR and scattering measurements, respectively. The temperature selected for all the measurements was 60 °C. D_2O solutions were used to avoid the IR spectral overlaps between Amide I band and strong ν_2 absorption band of water in the region 1650 cm^{-1}.

2.2. IR measurements

IR spectra were measured by using Bruker Vertex 70 spectrophotometer, equipped with a MIR light globar source (i.e. an U-shaped silicon carbide piece), with spectral resolution of 2 cm^{-1}. Each spectrum was averaged over 100 scans. All samples were placed between two CaF_2 windows, with a 0.05 mm Teflon spacer. The absorption spectrum of the empty beam line was subtracted from the spectrum of each sample. The resultant spectra were smoothed with a 13-point Savitzky and Golay function. In order to identify the time variations of each overlapping component under the broad amides, differential spectra were obtained by subtracting to the spectrum at a generic time t, the spectrum at t_0 (where t_0 was 7 minutes, for reaching thermal equilibrium).

2.3 Dynamic Light Scattering measurements

Zetasizer Nano-S90 (Malvern Instruments) Dynamic Light Scattering Instrument was used. It was equipped with a light source from a He–Ne laser (λ = 633 nm) and a scattering angle of 90°. The sample compartment was completely self enclosed and the temperature was automatically controlled. Temperature scanning was realized by increasing the temperature of 1 °C every 5 minutes and by starting measurement after an equilibration time of 3 minutes. The normalization of

the scattered intensity was done for each measurement. For polydisperse samples, the correlation function can be written as:

$$G(\tau) = A\left[1 + Bg_i(\tau)^2\right]$$

where A and B are the baseline and intercept of the correlation function and $g_i(\tau)$ is the sum of all the exponential decays exp-($2\Gamma\tau$), with $\Gamma = Dq^2$ and where D is translational diffusion coefficient and $q = (4\pi n/\lambda_0)\sin\theta/2$ (with n = refractive index of dispersant, λ_o = wavelength of the laser, θ = scattering angle). Two approaches are utilized to obtain size information from the correlation function: a) fitting a single exponential to the correlation function to obtain the mean size (z-average diameter); b) fitting a multiple exponential to the correlation function to obtain the distribution of particle sizes (such as CONTIN). The size distribution obtained is a plot of the relative intensity of light scattered by particles in various size classes and is therefore known as an intensity size distribution. Through Mie theory with the use of the input parameter of sample refractive index, it is possible to convert the intensity distribution to volume and number distributions [64,65].

3. Results and discussion

*** FIGURE 1 ***

Fig. 1 shows the temperature scanning of the scattered light for BLG native and in presence of metal ions (BLG, Cu-BLG and Zn-BLG). As can be seen, only in the Zn-BLG sample, it is evident a rapid increase of intensity, indicating an aggregation process that starts at about 48 °C. For the other two samples, BLG and Cu-BLG, nothing occurs until 60 °C. In view of the fact that for Zn-BLG over 60 °C the aggregation kinetic would be too fast, we have selected this temperature value to follow the aggregation kinetics for all the samples.

*** FIGURE 2 ***

To monitor the extent of the aggregation of all the samples we have performed scattering measurements as a function of time, as reported in Fig. 2. In particular, figure 2a reports the time

evolution of the total scattered intensity for all the three samples. It is relevant to note that, when the aggregation of Zn-BLG is finished, for the other two samples it is not still begun. In the Zn-BLG sample, better showed in the inset, after 10 minutes the total scattered intensity quickly increases for aggregation and after 70 minutes as much quickly decreases for precipitation. The total scattered intensities for BLG and Cu-BLG show behaviors very similar with a light increase for Cu-BLG with respect to that one of BLG, after 400 minutes. We think that this increased behavior, shown by Cu-BLG, with respect to BLG, is due to different conformational changes induced by the metal presence, or to the presence of the clusters of dense liquid (several hundred nanometers in size) which are metastable with respect to the protein solutions and the which formation takes place within a few seconds after sample preparation [66].

To evaluate the dimensions of the aggregates during the kinetics and to be sure that we are monitoring self-aggregation of the protein, we present, in Fig. 2b, the kinetics of the diameter mean dimension of molecular species which are present in the samples. It is evident how BLG and Cu-BLG, in these experimental conditions, follow similar evolution in the heat-induced aggregation, producing little species of about 200 nm of diameter (as better seen in the inset of the Fig. 2b), while Zn-BLG rapidly produces aggregates of about 4500/5000 nanometers of diameter. The discontinuity, shown by native BLG after 180 minutes, is not real but has to be attributed to the instrumental analysis and it is due to a superimposition of the correlation functions.

The analysis of these data, already discussed in paragraph 2.3, permits us to have the distribution of the diameters values with respect to particles numbers into solution and with respect to scattered intensity, at different time instants.

*** FIGURE 3 ***

In Fig. 3 we select the initial times (continuous line), considered the same zero time for all samples, and the final times (dashed line), different as a function of sample, being 11 hours for BLG and Cu-BLG (figs. 3a and 3b) and 50 minutes for Zn-BLG (fig. 3c). We observe that the results obtained for Cu-BLG and BLG are similar, i.e. both the samples produce aggregates of same value of size,

about 200 nm. On the contrary, Zn-BLG produces a biggest final size (up to 5000 nm) and a large amount of the aggregates in a shortest time, coherently with the data shown in Fig. 2.

*** FIGURE 4 ***

Analogously, we also show in Fig. 4 the distribution of the diameters values based on the intensity of the scattered light. Here, we report three times, those already shown in previous figure and an intermediate time (short dashed line) with respect to the complete time evolution for all samples. Once again the BLG and Cu-BLG are similar, while Zn-BLG has an aggregation kinetic very different. It is noteworthy that, for Cu-BLG and BLG in the intermediate time (figure 4a and 4b), the species are differently distributed with a main size around to 200 nm. This could explain the different increase of the scattered intensity shown by Cu-BLG in figure 2 with respect to the native protein as due to the presence of different species created by the presence of copper. For this reason, it results difficult to find a schematic model that explains the evolution of a so complex process.

To monitor changes in secondary (Amide I') and tertiary (Amide II) structures of protein with and without metal ions, we have performed kinetics of infrared absorption measurement for all the three samples.

We remind that Amide I is an infrared band attributed to an out of phase combination of C = O and C-N stretching of amide groups and that, in D_2O, it is called Amide I' for the shift towards 1650 cm^{-1}. Generally, Amide I' band has a composite profile, consisting of several spectral components related to different secondary structures [47].

*** FIGURE 5 ***

Fig. 5 shows the differential absorption spectra of the Amide I' band for all the three samples and highlights the time evolution of the main spectral components of the band. The spectral region between 1630 and 1650 cm^{-1} is attributed to α-helix, disordered random coil and intramolecular native β-sheet and, as it is evident, in all the samples decreases as a function of time (as indicated by arrows). It is noteworthy that the negative spectral component at 1640 cm^{-1} in the Cu-BLG sample is shifted towards 1635 cm^{-1}, usually assigned to native β-sheets structures and not

present in the other two samples. This shift indicates that a possible coordination of the copper, during the aggregation process, can produce different species, as already seen through light scattering. In BLG and Zn-BLG it is evident only a decrease without any shift and in Zn-BLG the component at 1650 cm^{-1} is present as a shoulder. The latter, attributed to α-helix and disordered structures, is probably less intense because of the specific coordination properties of zinc. Another negative contribution to the Amide I' band is present, at about 1690 cm^{-1} and assigned to native β-turn structures. We have already performed kinetic measurements of circular dichroism in the far-UV region with native BLG in similar conditions (buffer phosphate, lower concentration and 80 °C) and they showed that, already in the first minutes, native beta structures change in favor of other different type of beta structures [48]. Besides, all the samples present a conversion from α-helix and intramolecular β-native towards β-aggregated structures. In particular, the bands due to intermolecular aggregation are at around 1623 and 1685 cm^{-1} and are assigned to vibrations of strongly bound intermolecular β-strands and of anti-parallel β-sheet, respectively. In all the samples, these bands appear increased as a function of time, giving us the information that aggregation occurs, as seen also by light scattering. Then, the presence of copper determines an increase of the signal in the regions at about 1595 cm^{-1} and at about 1660 cm^{-1} with consequent lost of the isosbestic points, well defined in the native BLG sample. The spectral component at about 1590 cm^{-1} is attributed to asymmetric stretching of CO_2^-, when coordinated with Cu^{2+} [67].

A study realized on beta amyloid peptide has shown that zinc ion can bind one or two histidine, making itself available for further interaction; this may induce the formation of ordered aggregates, according to a model in which the metal plays the role of a bridge between the imidazole rings of two histidine residues possibly belonging to different peptides [3]. By the same study results that copper is tightly bound to three histidines of the same protein molecule in a closed structure, which ''protects'' the metal against any further interaction. More in general, the influence of metals in the higher or lower stabilization of native structure, after its coordination with histidines, is reported also for several native metallo-proteins. For example, in native enzyme SOD (superoxide

dismutase), that has the active site with the two metals, copper and zinc, the FTIR spectroscopy has revealed the influence of metals on the secondary structure of protein matrix [68]. From a comparison with our results, it is reasonable to think to a similar influence also in our samples.

*** FIGURE 6 ***

In Fig. 6, we have put together the Amide I' bands of all the three samples, at two different times, to better put in evidence the spectral differences shown in Fig. 5. As can be seen, the profiles of the differential spectra at the initial time are very similar for all the samples; after 5.5 hours, BLG and Zn-BLG show similar behaviors, indeed Cu-BLG shows changes principally in the two regions, at 1660-1680 and 1614 cm^{-1}. This suggest that Cu^{2+} influences the time evolution of the secondary structure of the native protein more than Zn^{2+}, which instead has a major influence on the time evolution of the aggregates building.

*** FIGURE 7 ***

In Fig. 7 are reported the kinetics of the differential absorption spectra in the Amide II and II' regions. Amide II band is attributed to an out-phase combination of in plane C-N stretching and N-H bending of Amide group. Time evolution of these bands gives us information on the protein partial unfolding with consequent H-D exchange between protein and solvent. The principal negative band at 1540 cm^{-1} and the positive band at 1436 cm^{-1}, that are probes of H-D exchange, are present in all the samples. Once again, it results evident that the partial opening of the protein at initial times of the aggregation is necessary [47]. Then, there is a band at about 1442 cm^{-1} present only in Cu-BLG, which is probably attributed to the presence and coordination of copper with protein.

*** FIGURE 8 ***

Summarizing the spectral details, in Fig. 8 we report the time evolution of the component of Amide I' band at 1623 cm^{-1} for the three samples (8a) and at 1614 cm^{-1} only for Cu-BLG (8b) and of the component of Amide II' at 1436 cm^{-1} for all investigated samples (8c). For the three samples, we observe the formation of β-aggregated structures through the increase of the spectral component

at 1623 cm^{-1}. It is noteworthy to underline that for Cu-BLG the different behavior of the spectral component at 1623 cm^{-1} is due to the competitive appearance of the spectral component at 1614 cm^{-1}, after about 45 minutes, thus confirmed in Fig. 8b by the presence of two different trends. This last spectral component is attributed to the formation of very strong intermolecular H-bonds [44,60,69] and we suggest that the specific presence of copper may promote, in a very short time, the formation of heat-induced network ready to form macromolecules and/or gels, as reported for many globular protein, such as BLG [70,71]. As it is shown in Fig. 8c, it is evident that the presence of metals in solution affects in a different way the rate and the time evolution of the protein partial unfolding. Moreover, we outline that for Zn-BLG the partial unfolding of the protein seems to stop after 120 minutes, time in which the bigger aggregates are formed, as already reported in figure 2b. Indeed, for BLG and Cu-BLG the contemporary processes of opening and aggregation, at this temperature, are longer, being less pronounced in Cu-BLG, as already seen in the inset of figure 2b. These behaviors confirm us the existence of contemporary steps like conformational opening due to tertiary structure changes, like structural changes due to secondary structures changes, induced also by the coordination with metal ions, and like intermolecular interactions that can select to go towards aggregation and/or gelation process. The Cu-BLG conformation, in our conditions, has some structural changes, due also to the specific coordination with the ion, and some intermolecular interactions that drive the aggregates towards the formation of the gel texture.

4. Conclusion

The results, shown and discussed in this paper, highlight that metal ions affect the tertiary and secondary structure changes and the formation of supramolecular aggregates in BLG. We outline that Cu^{2+} and Zn^{2+} play a different role in conditioning the time evolution of the heat-induced aggregation process. In particular, Cu^{2+} influences mainly the time evolution of the protein secondary structure and of its initial conformational changes, inducing the formation of stronger H-linked bonds but not influencing the trend of aggregates formation. Instead, Zn^{2+} presents similar

changes of the conformational and structural changes with respect to the BLG without metal ions, but dramatically influences the formation of big aggregates in a shorter time.

Summarizing the details, conformational and structural changes are the dominant initial steps that drive the aggregation process. In particular, the initial partial opening of the tertiary structures (monitored by Amide II region) and the structural changes between native secondary structures and β–aggregates (monitored by Amide I') occur in all the three samples, BLG, Cu-BLG and Zn-BLG. Following aggregation kinetics, a common trend comes out: at fixed temperature, as time increases, gradually β–aggregates structures increase and ordered α–helix and native β–structures decrease. The presence of metal ions in solution influences these structural changes, due to different coordination of the two metal ions here studied. The presence of zinc ion induces the formation of big size (until to 5000 nm of diameter) aggregates in larger amount, in very short time and in a lower temperature. The presence of copper ion, indeed, destabilizes also some native β–structures not evidenced neither in BLG nor in Zn-BLG (as showed by the shift at 1635 cm^{-1}); in fact, copper ion has an own coordination that involves different conformational changes during the aggregation process (as showed by bands at 1660, 1590 and 1445 cm^{-1} present only in this sample). The presence of β–aggregates of small dimensions (monitored by band at 1623 and 1685 cm^{-1}) together with copper ion seems to favor the formation of very strong intermolecular H-bonds (monitored by band at 1614 cm^{-1}) not present in the other samples. This behavior, as reported in literature, is attributed to the initial formation of a network of bonds that can take towards gelation. As it is known, for example cold gelation consists in a pre-heating of the sample and its subsequent cooling that takes to the gel formation. Our data suggest that, during the heating, pre-aggregates of Cu-BLG can select an alternative patch than that one of aggregation: the patch of the formation of a network of H-bonds that takes towards the gelation.

It will be very interesting to continue to investigate when and why Cu-BLG prefers to go towards the gelation rather than towards formation of larger aggregates and how this depends by

external solvent, conditions and also by the type of protein. This is an open road to explore and to use in various applied fields.

References

[1] M.A. Lovell, J.D. Robertson, W.J. Teesdale, J.L. Campbell & W.R. Markesbery, Copper, iron and zinc in Alzheimer's disease senile plaques. J Neurol Sci 158, (1998) 47–52.

[2] D.Religa, D.Strozyk, R.A.Cherny, I.Volitakis, V. Haroutunian, B. Winblad, J. Naslund & A. I. Bush, Elevated cortical zinc in Alzheimer disease. Neurology 67, (2006) 69–75.

[3] F. Stellato, G. Menestrina M. Dalla Serra, C. Potrich, R. Tomazzolli, W. Meyer-Klaucke S. Morante, Metal binding in amyloid β-peptides shows intra- and inter-peptide coordination modes. Eur Biophys J (2006) 35: 340–351.

[4] L. Wang, W. Colon, Effect of Zinc, Copper and Calcium on the Structure and Stability of Serum Amyloid A. Biochemistry 46(18), (2007) 5562-5569.

[5] L. O. Tjernberg, D. J. E. Callaway, A Tjernberg, S. Hahne, C. Lilliehook, L. Terenius, J. Thyberg and C. Nordstedt, A Molecular Model of Alzheimer Amyloid β-Peptide Fibril Formation. J. Biol. Chem. 274 (1999), 12619-12625.

[6] J. Danielsson, R. Pierattelli, L. Banci and A. Graslund, High-resolution NMR studies of the zinc-binding site of the Alzheimer's amyloid b-peptide. FEBS Journal 274, (2007) 46–59.

[7] A. I. Bush, W. H. Pettingell, G. Multhaup, M. d'Paradis, J. P. Vonsattel, J. F. Gusella, K. Beyreuther, C. L. Masters & R. E. Tanzi, Rapid induction of Alzheimer A beta amyloid formation by zinc. Science 265, (1994) 1464–1467.

[8] B. Raman, T. Ban, K. Yamaguchi, M. Sakai, T. Kawai, H. Naiki & Y. Goto, Metal ion-dependent effects of clioquinol on the fibril growth of an amyloid {beta} peptide. J Biol Chem 280, (2005) 16157–16162.

[9] X. Huang, C. S. Atwood, R. D. Moir, M. A. Hartshorn, J. P. Vonsattel, R. E. Tanzi & A. I. Bush, Zinc-induced Alzheimer's Abeta1–40 aggregation is mediated by conformational factors. J Biol Chem 272, (1997) 26464–26470.

[10] M. Comai, M. Dalla Serra, C. Potrich , G. Menestrina, Cu2+ and Zn2+ effects on beta-amyloid aggregation and structural conformation. Biophys J 84:337a (2003).

[11] K. Suzuki, T. Miura and H. Takeuchi, Inhibiyory Effect of Copper(II) on Zinc(II)- induced Aggregation of Amyloid b-Peptide. Biochem. Biophys. Res. Commun. 285 (2001), 991-996.

[12] C. S. Atwood, R. D. Moir, X. Huang, R. C. Scarpa, N. M. Bacarra, D. M. Romano, M. A. Hartshorn, R. E. Tanzi & A. I. Bush. Dramatic aggregation of Alzheimer aβ by Cu(II) is induced by conditions representing physiological acidosis. J. Biol. Chem. 273, (1998) 12817–12826.

[13] T. Miura, K. Suzuki, N. Kohata & H. Takeuchi, Metal Binding Modes of Alzheimer's Amyloid β-Peptide in Insoluble Aggregates and Soluble Complexes. Biochemistry 39 (2000), 7024–7031.

[14] Y. Yoshiike, K. Tanemura, O. Murayama, T. Akagi, M. Murayama, S. Sato, X. Sun, N. Tanaka & A. Takashima, New insights on how metals disrupt amyloid beta-aggregation and their effects on amyloid-beta cytotoxicity. J. Biol. Chem. 276, (2001) 32293–32299.

[15] A. M. Brown, D. M. Tummolo, K.J. Rhodes, J. R. Hofmann, J. S. Jacobsen & J. Sonnenberg-Reines, Selective aggregation of endogenous beta-amyloid peptide and soluble amyloid precursor protein in cerebrospinal fluid by zinc. J. Neurochem. 69, (1997) 1204–1212.

[16] E. House, J. Collingwood, A. Khan, O. Korchazkina, G. Berthon & C. Exley, Aluminium, iron, zinc and copper influence the in vitro formation of amyloid fibrils of Aβ42 in a manner which may have consequences for metal chelation therapy in Alzheimer's disease. J. Alzheimer's Dis. 6, (2004) 291–301.

[17] K. Garai, P. Sengupta, B. Sahoo, S. Maiti, Selective destabilization of solubile β oligomers by divalent metal ions. Biochem. Biophys. Res. Commun. 354, (2006) 210-215.

[18] J. P. Cleary, D. M. Walsh, J. J. Hofmeister, G.M. Shankar, M. A. Kuskowski, D. J. Selkoe & K. H. Ashe, Natural oligomers of the amyloid-β protein specifically disrupt cognitive function. Nat. Neurosci. 8, (2005) 79–84.

[19] M.A. Westerman, D. Cooper-Blacketer, A. Mariash, L. Kotilinek, Kawarabayashi T, L. H. Younkin, G. A. Carlson, S. G. Younkin & K. H. Ashe. The relationship between Aβ and memory in the Tg2576 mouse model of Alzheimer's disease. J Neurosci 22, (2002) 1858–1867.

[20] D. J. Selkoe, Cell biology of protein misfolding: the examples of Alzheimer's and Parkinson's diseases. Nat. Cell. Biol. 6, (2004) 1054–1061.

[21] M. Hoshi, M. Sato, S. Matsumoto, A. Noguchi, K. Yasutake, N. Yoshida & K. Sato Spherical aggregates of β-amyloid (amylospheroid) show high neurotoxicity and activate tau protein kinase I/ glycogen synthase kinase- 3beta. Proc. Natl. Acad. Sci. USA 100, (2003) 6370–6375.

[22] S. Lesne´, M. T. Koh, L. Kotilinek, R. Kayed, C. G. Glabe, A. Yang, M. Gallagher & K. H. Ashe, A specific amyloid-beta protein assembly in the brain impairs memory. Nature 440, (2006) 352–357.

[23] D. M. Walsh, I. Klyubin, G. M. Shankar, M. Townsend, J. V. Fadeeva, V. Betts, M. B. Podlisny, J. P. Cleary, K. H. Ashe , M. J. Rowan et al. The role of cell-derived oligomers of Abeta in Alzheimer's disease and avenues for therapeutic intervention. Biochem. Soc. Trans. 33, (2005) 1087–1090.

[24] R. Carrotta, M. Di Carlo, M. Manno, G. Montana, P. Picone, D. Romancino, and P. L. San Biagio, Toxicity of recombinant {beta}-amyloid prefibrillar oligomers on the morphogenesis of the sea urchin Paracentrotus lividus. FASEB J. 20, (2006) 1916-1917.

[25] J. Dong, C. S. Atwood, V. E. Anderson, S. L. Siedlak, M. A. Smith, G. Perry & P. R. Carey, Metal binding and oxidation of amyloid-beta within isolated senile plaque cores: Raman microscopic evidence. Biochemistry 42, (2003) 2768–2773.

[26] Y. Mekmouche, Y. Coppel, K. Hochgrafe, L. Guilloreau, C. Talmard, H. Mazarguil & P. Faller, Characterization of the ZnII binding to the peptide amyloidβ1–16 linked to Alzheimer's disease. Chem. Biochem. 6, (2005) 1663–1671.

[27] S. Zirah, S. A. Kozin, A. K. Mazur, A. Blond, M. Cheminant, I. Segalas-Milazzo, P. Debey & S. Rebuffat, Structural changes of region 1–16 of the Alzheimer disease amyloid beta-peptide upon zinc binding and in vitro aging. J. Biol. Chem. 281, (2006) 2151–2161.

[28] S. Zirah, R. Stefanescu, M. Manea, X. Tian, R. Cecal, S. A. Kozin, P. Debey, S. Rebuffat & M. Przybylski, Zinc binding agonist effect on the recognition of the β-amyloid (4–10) epitope by anti-beta-amyloid antibodies. Biochem. Biophys. Res. Commun. 321, (2004) 324–328.

[29] S. Morante, R. Gonzalez-Iglesias, C. Potrich, C. Meneghini, W. Meyer-Klaucke, G. Menestrina and M. Gasset, Inter- and Intra-octarepeat Cu(II) Site Geometries in the Prion Protein: implications in Cu(II) binding cooperativity and Cu(II)-mediated assemblies. J. Biol. Chem. 279 (2004), 11753–11759.

[30] C. D. Syme, R. C. Nadal, S. E. Rigby & J. H. Viles, Copper binding to the amyloid-β (Ab) peptide associated with Alzheimer's disease: folding, coordination geometry, pH dependence, stoichiometry, and affinity of Aβ-(1–28): insights from a range of complementary spectroscopic techniques. J. Biol. Chem. 279, (2004)18169–18177.

[31] W. Garzon-Rodriguez, A. K. Yatsimirsky & C. G. Glabe, Binding of Zn(II), Cu(II), and Fe(II) ions to Alzheimer's A-beta peptide studied by fluorescence. Bioorg. Med. Chem. Lett. 9, (1999) 2243–2248.

[32] A. I. Bush & R. E. Tanzi, The galvanization of beta-amyloid in Alzheimer's disease. Proc. Natl. Acad. Sci. USA 99, (2002) 7317–7319.

[33] A. P. Smith, M. N. Lee, Role of zinc in ALS. Amyotroph Laterral Scler 3, (2007) 131-143.

[34] T. Sakiyama, A. Ava, M. Embutsu, K. Imamura, K. Nakanishi, Protease susceptibility of beta-lactoglobulin adsorbed on stainless steel surface as evidence of contribution of its specific segment to adsorption. J. Biosci. Bioeng 101, (2006) 434-4391.

[35] H. Singh, A. Flynn, P. F. Fox, Binding of zinc to bovine and human milk proteins. J. Dairy Sci. 72, (1989) 235-248.

[36] J. E. O'Connell, P. F. Fox, Effect of beta-lactoglobulin and precipitation of calcium phosphate on the thermal coagulation of milk. J. Dairy Res. 68, (2001) 81-94.

[37] S. G.Bolder, H.Hendrickx, L. M. C.Sagis, E. van der Linden, Fibril assemblies in aqueous whey protein mixtures. J. Agric. Food Chem. 54, (2006) 4229-4234.

[38] C.Veerman, L. M. C. Sagis, J. Heck, E. van der Linden, Mesostructure of fibrillar bovine serum albumin gels. Int. J. Biol. Macromol. 31, (2003) 139-146.

[39] R. Ipsen, J. Otte, K. B. Ovist, Molecular self-assembly of partially hydrolysed alpha-lactalbumin resulting in strong gels with a novel microstructure. J. Dairy Res. 68, (2001) 277-286.

[40] J. W. Simons, H. A. Kosters, R. W. Visschers, H. H. de Jongh, Role of calcium as trigger in thermal beta-lactoglobulin aggregation. Arch. Biochem. Biophys. 406, (2002) 143-152.

[41] S. Saeseaw, J. Shiowatana, A. Siripinyanond, Observation of salt-induced beta-lactoglobulin aggregation using sedimentation field-flow fractionation. Anal. Bioanal. Chem. 386, (2006) 1681-1688.

[42] S. Bouhallab, G. Henry, F. Caussin, J. Croguennec, J. Fauquant, D. Mollès, Copper-catalyzed formation of disulfide-linked dimer of bovine β-lactoglobulin. Lait 84 (2004), 517-525.

[43] B. J. Harvey, E. Bell and L. Brancaleon, A Tryptophan Rotamer Located in a Polar Enviroment Probes pH-Dependent Conformational Changes in Bovine b-Lactoglobulin A. J. Phys. Chem. B, 111, (2007) 2610-2620.

[44] G. E. Remondetto, M. Subirade, Molecular Mechanisms of Fe^{2+}-Induced β- Lactoglobulin Cold Gelation. Biopolymers, Vol. 69, (2003) 461-469.

[45] F. G. Pearce, S. H. Mackintosh, J. A. Gerrard, Formation of amyloid-like fibrils by Ovalbumin and related proteins under conditions relevant to food processing. J. Agric. Food Chem. 55, (2007) 318-322.

[46] V. Militello, V. Vetri, M. Leone, Conformational changes involved in thermal aggregation processes of Bovine Serum Albumin, Biophys. Chem. 105, (2003) 133–141.

[47] V. Militello, C. Casarino, A. Emanuele, A. Giostra, F. Pullara, M. Leone, Aggregation kinetics of bovine serum albumin studied by FTIR spectroscopy and light scattering, Biophys. Chem. 107, (2004) 175–187.

[48] V. Vetri, V. Militello, Thermal induced conformational changes involved in the aggregation pathways of beta-lactoglobulin. Biophys. Chem. 113 (2005) 83-91.

[49] V. Vetri, F. Librizzi, M. Leone, V. Militello, Thermal aggregation of bovine serum albumin at different pH: comparison with human serum albumin. Eur. Biophys. J. DOI: 10.1007/s00249-007-0196-5.

[50] V. Vetri, C. Canale, A. Relini, F. Librizzi, V. Militello, A. Ghiozzi, Amyloid fibrils formation and amorphous aggregation in Concanavalin A. Biophys. Chem. 125, (2007) 184-190.

[51] W. L. Chen, M. T. Hwang, C. Y. Liau, J. C. Ho, K. C. Hong, S. J. Mao, Beta-lactoglobulin is a thermal marker in processed milk as studied by electrophoresis and circular dichroic spectra. J. Dairy Sci. 88, (2005) 1618-1630.

[52] G. Kontopidis, C. Holt, and L. Sawyer, β-Lactoglobulin: Binding Properties,Structure, and Function. J. Dairy Sci. 87, (2004) 785–796.

[53] Perla Relkin, Reversibility of heat-induced conformational changes and surface exposed hydrophobic clusters of β-lactoglobulin: their role in heat-induced sol–gel state transition. Int. J. Biol. Macromol. 22, (1998) 59–66.

[54] M.Z. Papiz, L. Sawyer, E.E. Eliopoulos, A.C.T. North, J.B.C. Findlay, R. Sivaprasadarao, T.A. Jones, M.E. Newcomer, P.J. Kraulis, The structure of β-lactoglobulin and its similarity to plasma retinol-binding protein. Nature 324, (1986) 383– 385.

[55] T.V. Burova, N.V. Grinberg, R.W. Visschers, V.Y. Grinberg, C.G. De Kruif, Thermodynamic stability of porcine β-lactoglobulin. A structural relevance. Eur. J. Biochem. 269, (2002) 3958–3968.

[56] S. Uhrinova, M.H. Smith, G.B. Jameson, D. Uhrin, L. Sawyer, P.N. Barlow, Structural changes accompanying pH-induced dissociation of the beta-Lactoglobulin dimer. Biochemistry 39, (2000) 3565– 3574.

[57] S. Cairoli, S. Iametti, F. Bonomi, Reversible and irreversible modifications of β-lactoglobulin upon exposure to heat. J. Protein Chem. 13, (1994) 347–354.

[58] L. Monaci and A.J. van Hengel, Effect of Heat Treatment on the Detection of Intact Bovine β-Lactoglobulins by LC Mass Spectrometry. J. Agric. Food Chem. 55, (2007) 2985-2992.

[59] H. C. Liu, W. L. Chen, S. J. Mao, Antioxidant nature of bovine milk beta-lactoglobulin. J. Dairy Sci. 90, (2007) 547-555.

[60] A. F. Allain, P. Paquin, M. Subirade, Relationships between conformation of β-lactoglobulin in solution and gel states as revealed by attenuated total reflection Fourier transform infrared spectroscopy. Int. J. Biol. Macrom. 26, (1999) 337–344.

[61] A. Dong, J Matsuura, M. C. Manning and J. F. Carpenter, Intermolecular β-Sheet Results from Trifluoroethanol-Induced Nonnative a-Helical Structure in β-Sheet Predominant Proteins: Infrared and Circular Dichroism Spectroscopic Study. Arch. Biochem. Biophys. Vol. 355, No. 2, (1998) 275–281.

[62] S.R. Paik, H.J. Shin, J.H. Lee, C.S. Chang and J. Kim, Copper(II)-induced self-oligomerization of α-synuclein. Biochem. J. 340, (1999) 821–828.

[63] D. Renard, J. Lefebvre, P. Robert, G. Llamas, E. Dufour, Structural investigation of β-lactoglobulin gelation in ethanol/water solutions. Int. J. Biol. Macromol. 26, (1999) 35–44.

[64] G. Mie, Beitrage zur optik truber medien, speziell kolloidaler metallosungen. Ann. Phys. 25, (1908) 377–445.

[65] C. F. Bohren, and D. R. Huffman, "Absorption and Scattering of Light by Small Particles", Wiley, New York, 1983.

[66] W. Pan, O. Galkin, L. Filobelo, R. L. Nagel and P. G. Vekilov, Metastable Mesoscopic Clusters in Solutions of Sickle-Cell Hemoglobin. Biophys. J. 92, (2007) 267–277.

[67] J. G. Mesu, T. Visser, F. Soulimani, E. E. van Faassen, P. de Peinder, A. M. Beale and B. M. Weckhuysen, New Insights into the Coordination Chemistry and Molecular Structure of Copper(II) Histidine Complexes in Aqueous Solutions. Inorg. Chem. 45, (2006) 1960-1971.

[68] W. Y. Sun, J. L. Fang, M. Cheng, P. Y. Xla, W. X. Tang, Secondary Strucutre Dependent on Metal Ions of Copper, Zinc Superoxide Dismutase Investigated by Fourier Transform IR Spetroscopy. Biopolymers 42, (1997) 297–303.

[69] M. Jackson, H. H. Mantsch, Halogenated alcohols as solvents for protein: FTIR spectroscopic studies. Biochim Biophys Acta 1118, (1992) 139–143.

[70] D. M. Mulvihill, J. E. Kinsella, Gelation characteristics of whey proteins and β–Lactoglobulin. Food Technol. 41, (1987) 102-111.

[71] G. R. Ziegler, E. A. Foegeding, Gelation of proteins. Adv. Food Nutr. Res.. 34, (1990) 203-298.

Figure Captions

Figure 1: Normalized scattered intensity as a function of temperature for (□) BLG, (○) Cu-BLG and (Δ) Zn-BLG.

Figure 2: (a) Time evolution of the normalized scattered intensity and (b) of the average diameter of (□) BLG, (○) Cu-BLG and (Δ) Zn-BLG at T = 60°C. Inset in (a) shows a zoom for the first 60 minutes. Inset in (b) shows a zoom for BLG and Cu-BLG.

Figure 3: Size distribution of aggregates dimension based on the numbers of particles present into solution at initial (t_0) and final time (t_f) of the scattering kinetic, at T = 60°C: (up) BLG, t_0 = 0 (continuous line) and t_f = 11 hours (dashed line), (middle) Cu-BLG, (bottom) Zn-BLG with t_f = 50 minutes (dashed line).

Figure 4: Size distribution of aggregates dimension based on the intensity of light scattered, at T = 60°C; times and lines as in figure 4 with addition of t_m = 5.5 hours for BLG and Cu-BLG and t_m = 20 minutes for Zn-BLG (short dashed lines): (up) BLG, (middle) Cu-BLG, (bottom) Zn-BLG.

Figure 5: Infrared absorption differential spectra in the Amide I' region, defined as $\Delta A(t) = A(t) - A(t = 0)$; (a) BLG, (b) Cu-BLG, (c) Zn-BLG. All the measurements are made at T = 60°C.

Figure 6: FTIR differential spectra for BLG (continuous line), Cu-BLG (long dashed line), and Zn-BLG (short dashed line), at two times 10 minutes (initial time after thermal equilibrium, dark spectra) and 5.5 hours (light grey spectra).

Figure 7: Time evolution of infrared absorption differential spectra in the Amide II and Amide II' region, defined as $\Delta A(t) = A(t) - A(t = 0)$; (a) BLG, (b) Cu-BLG, (c) Zn-BLG. All the measurements are made at T = 60°C.

Figure 8: Time evolution of the differential absorption intensity of Amide I' components: (a) at 1623 cm^{-1} for (□) BLG, (○) Cu-BLG, (Δ) Zn-BLG and (b) at 1614 cm^{-1} for only Cu-BLG; (c) time evolution of the differential absorption intensity of Amide II' component at 1436 cm^{-1}. Error bar

showed at the top on the right of (a) is the experimental error estimated for differential absorption values.

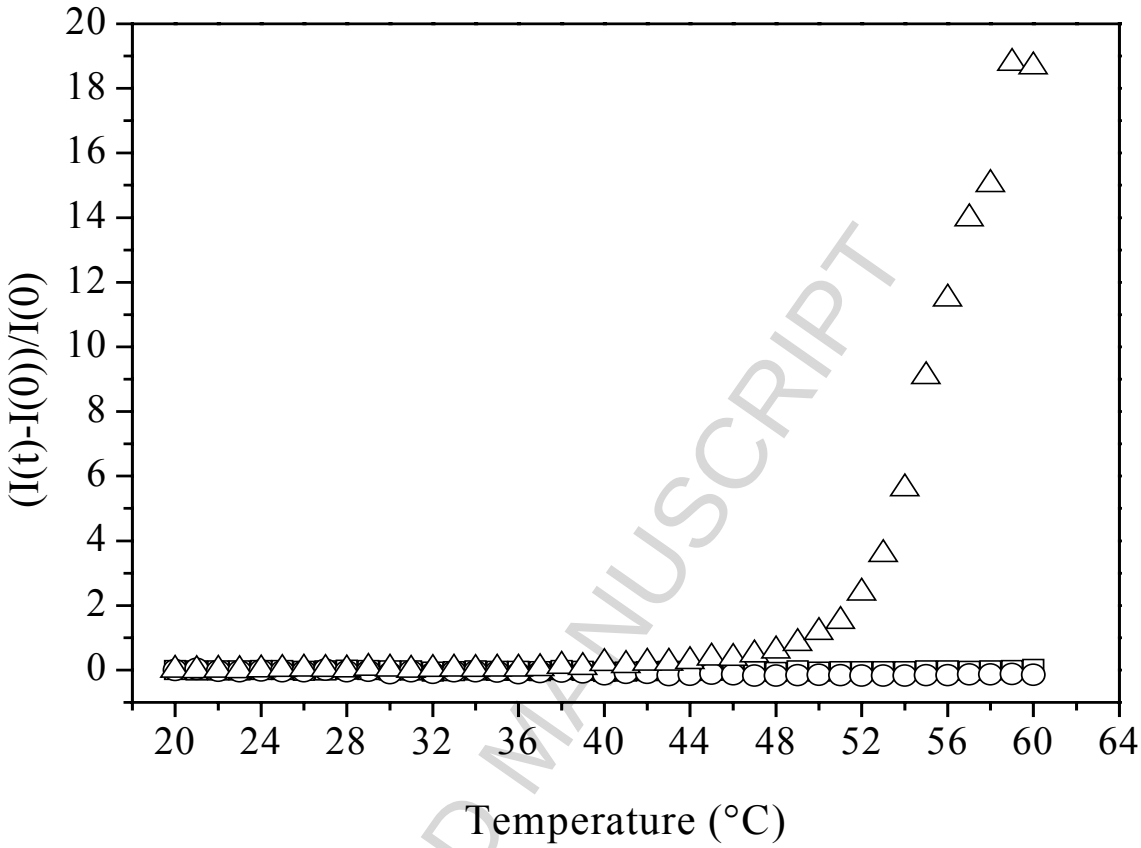

Figure 1

Navarra et al.

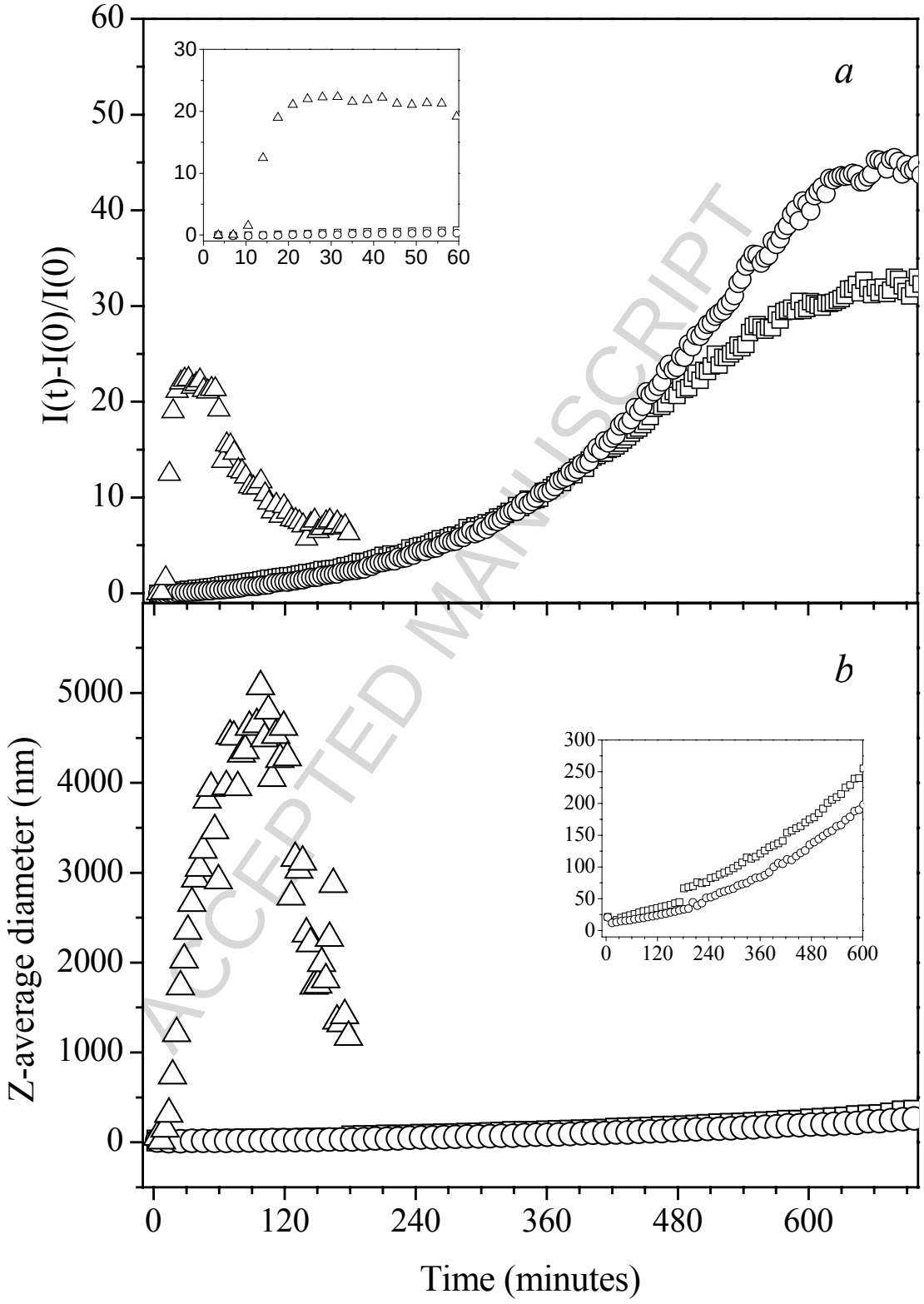

Figure 2
Navarra et al.

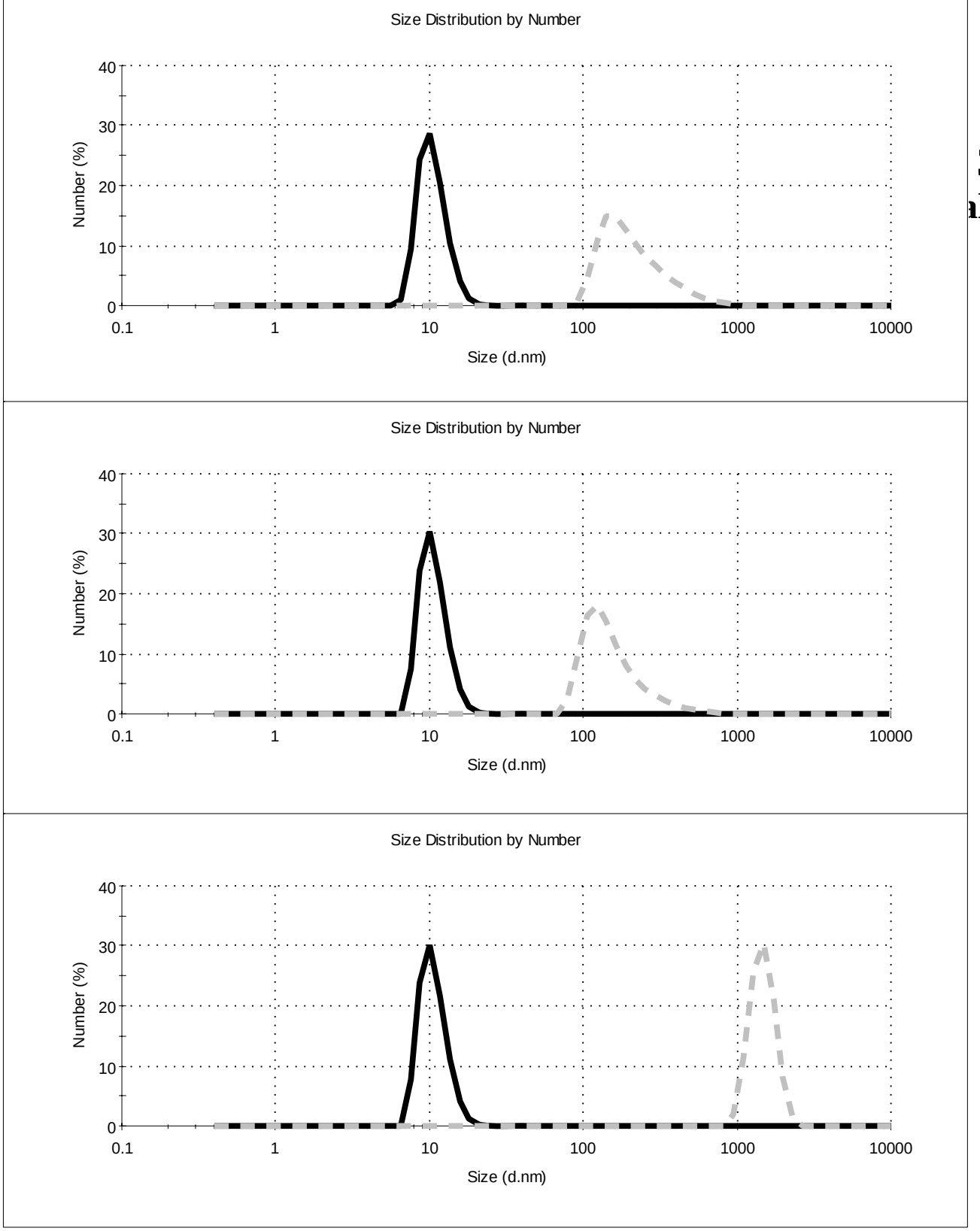

Figure 3
Navarra et al.

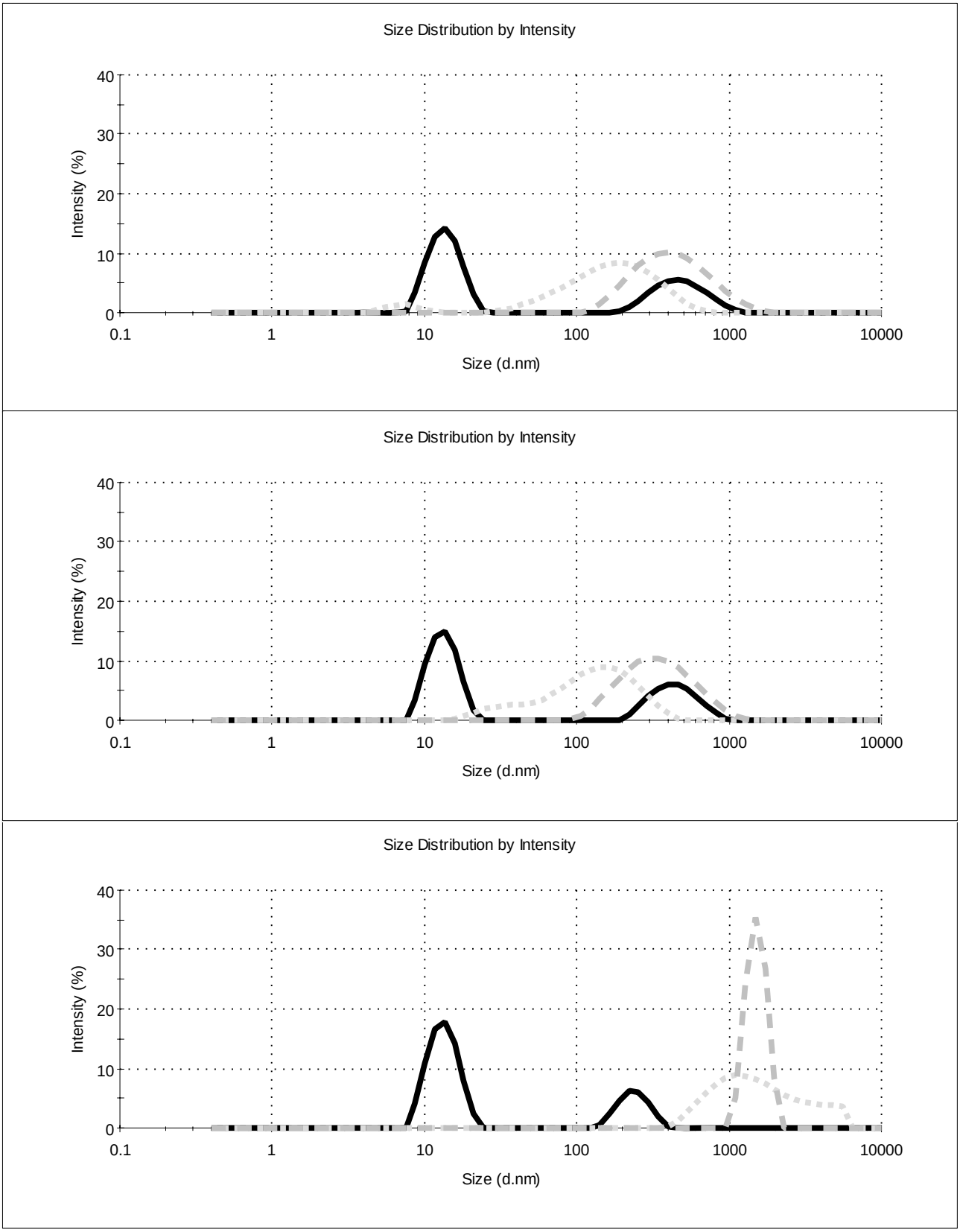

Figure 4
Navarra et al.

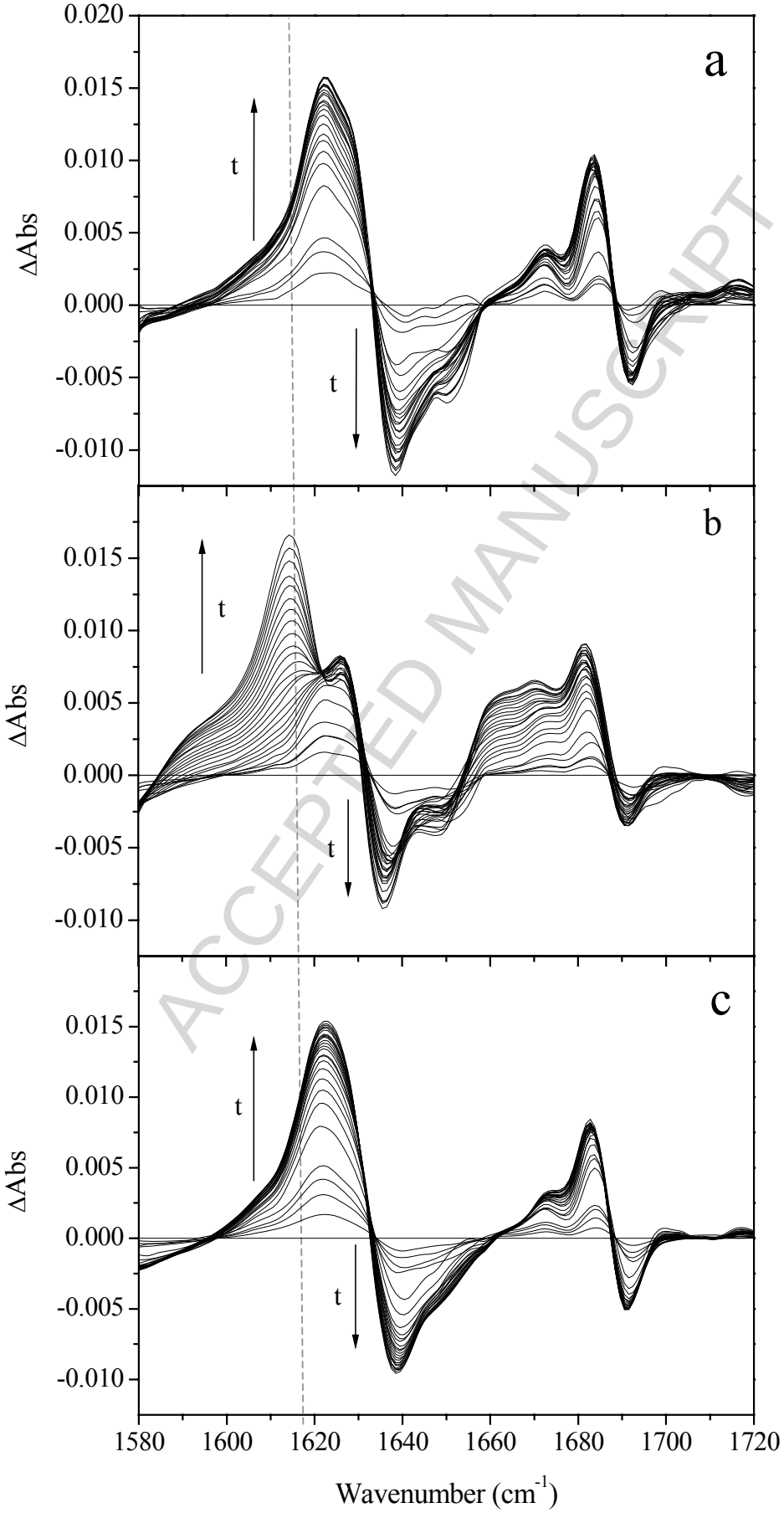

Figure 5
Navarra et al.

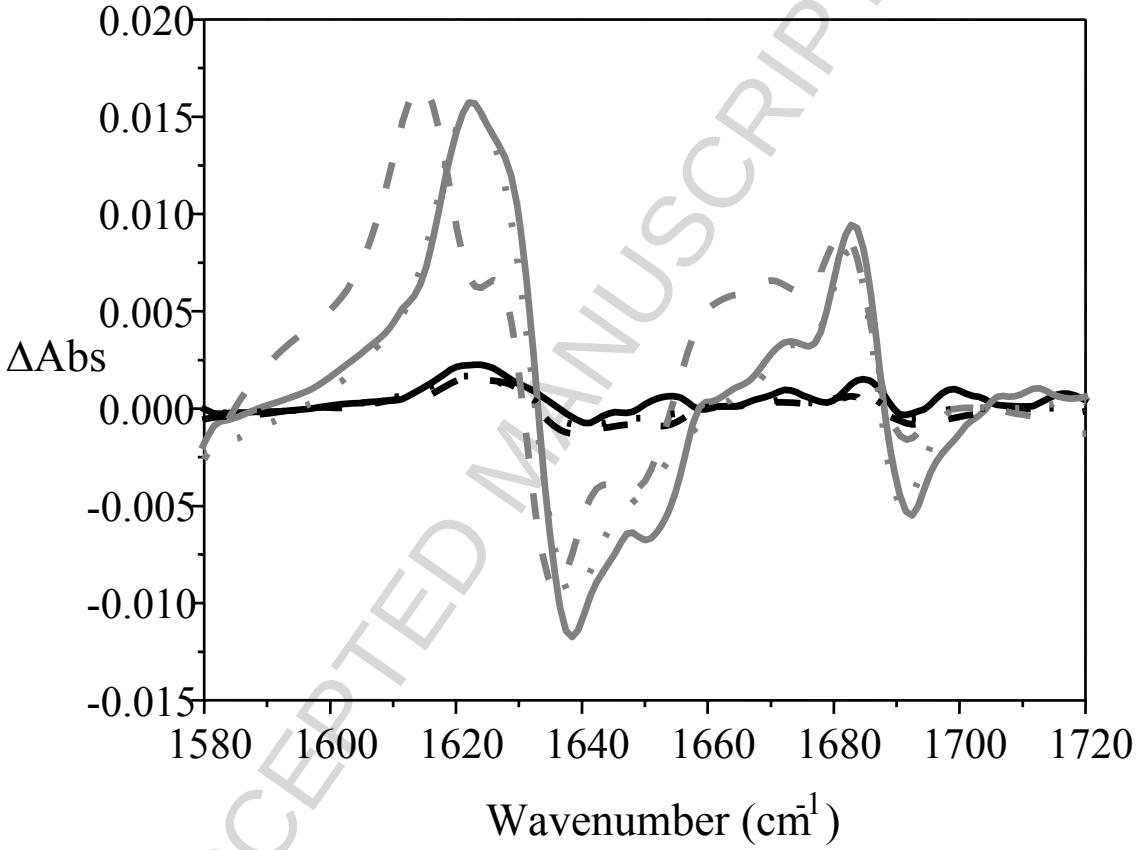

Figure 6
Navarra et al.

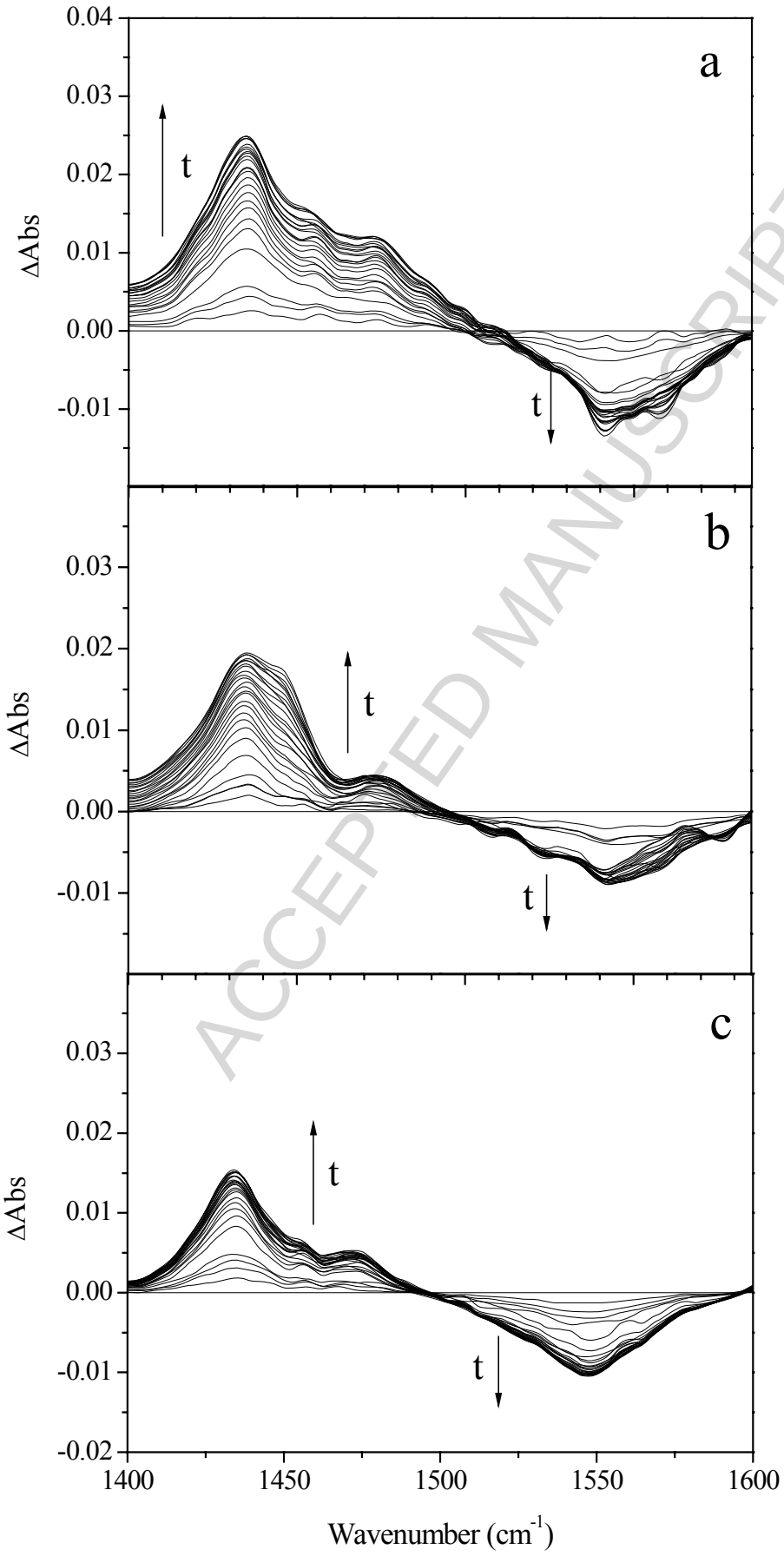

Figure 7
Navarra et al.

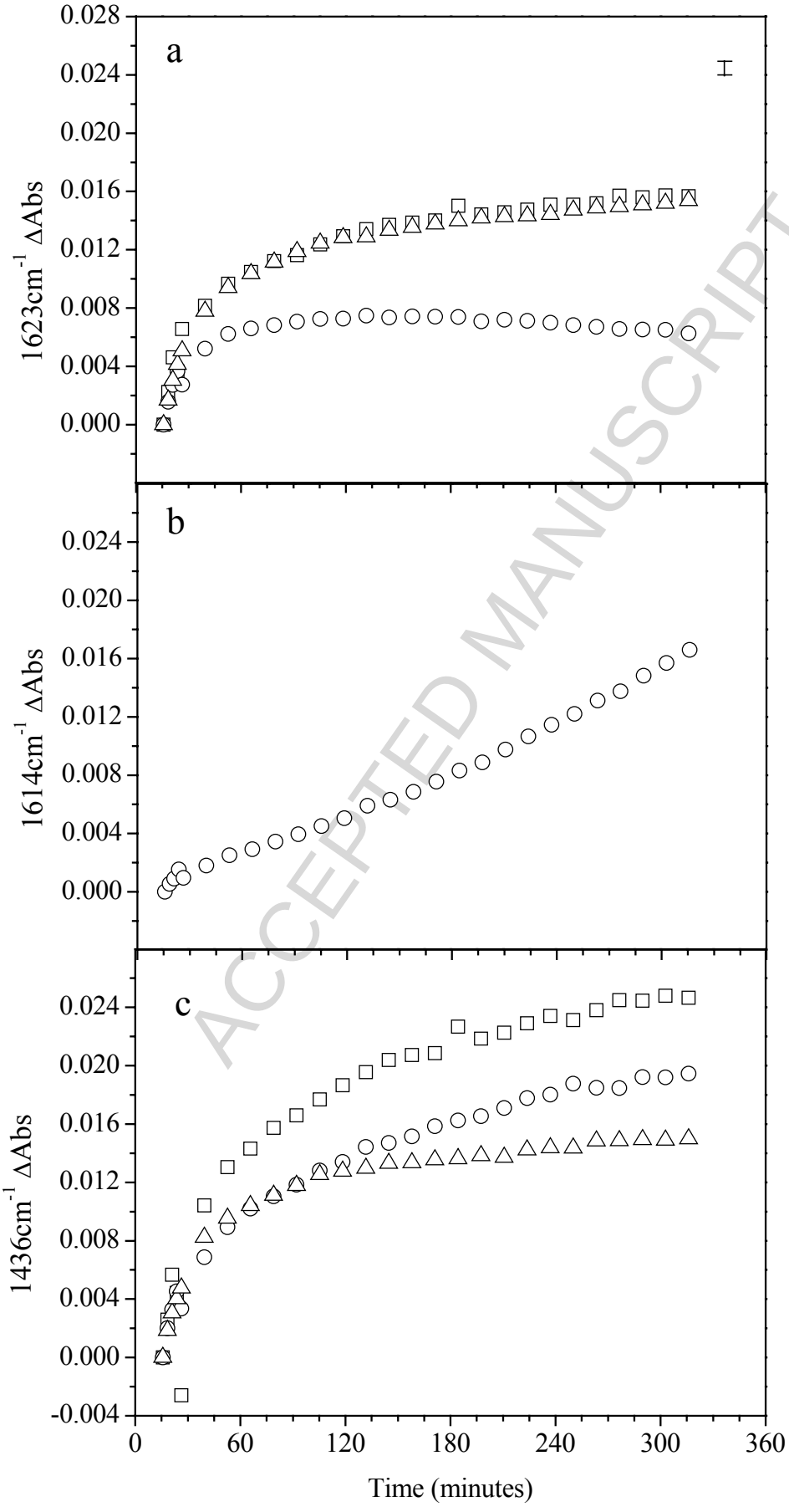

Figure 8
Navarra et al.